# Early development of self-administered COVID-19 rapid test based on nucleocapsid detection in saliva sample

Siti Soidah[1], Toto Subroto[2,3], Sari Syahruni[3], Fauzian Giansyah[3], Henry Chandra[3], Dhiya Salsabila[3], Bachti Alisjahbana[4], Nisa Fauziah[5], Hesti Lina Wiraswati[5], Leonardus Widyatmoko[6], Basti Andriyoko[6], Anita Yuwita[7], Muhammad Yusuf[2,3,*]

[1]Master of Biotechnology Program, School of Postgraduates, Universitas Padjadjaran, Jl. DipatiUkur 35 Bandung, West Java 40132, Indonesia
[2]Department of Chemistry, Faculty of Mathematics and Natural Sciences, Universitas Padjadjaran, Jl. Raya Bandung-Sumedang Km 21, Jatinangor, Sumedang, West Java 45363, Indonesia
[3]Research Center for Molecular Biotechnology and Bioinformatics, Universitas Padjadjaran, Jl.Singaperbangsa 2 Bandung, West Java 40132, Indonesia
[4]Department of Internal Medicine, Faculty of Medicine, Universitas Padjadjaran, Hasan Sadikin Hospital, Jl. Pasteur No.38 Bandung, West Java 40161, Indonesia
[5]Department of Biomedical Sciences, Parasitology Division, Faculty of Medicine Universitas Padjadjaran, Jl. Raya Bandung-Sumedang Km 21, Jatinangor, Sumedang, West Java 45363, Indonesia
[6]Department of Clinical Pathology, Faculty of Medicine, Universitas Padjadjaran, Hasan Sadikin Hospital, Jl. Pasteur No.38 Bandung, West Java 40161, Indonesia
[7]Research and Development Division, PT. Pakar Biomedika, Jl. Rancabentang No.12B Ciumbuleuit, Bandung, West Java 40142, Indonesia
*Corresponding author: m.yusuf@unpad.ac.id

**ABSTRACT** More than 6,000,000 people have died due to the coronavirus (COVID-19) pandemic. This disease spread quickly due to its highly contagious nature. The SARS-CoV-2 virus that causes the disease can be transmitted through saliva droplets secreted by infected people at a distance of less than 1 m. As a result, saliva has been accepted as an alternative specimen for COVID-19 detection by the Centers for Disease Control and Prevention (CDC). Furthermore, WHO recommended the use of rapid antigen tests based on lateral flow immunoassay when reverse transcription-polymerase chain reaction (RT-PCR) is not available. We developed a saliva-based rapid antigen test by optimizing the antibody concentration and optimum pH for the conjugation of antibody and gold nanoparticles. We found that the best running buffer formulation consisted of 75 mM sodium phosphate buffer, 1% NaCl, 1% Triton X-100, 0.5% N-acetyl-L-cysteine, and 0.02% sodium azide. The addition of a mucolytic agent in the buffer can reduce the viscosity of saliva, thus improving sensitivity. The rapid test developed detected the lowest concentration of nucleocapsid protein at 0.1 µg/mL. Our study revealed 100% specificity against negative COVID-19 saliva and no cross-reaction with avian influenza virus hemagglutinin.

**KEYWORDS** lateral flow immunoassay; rapid antigen test; saliva; SARS-CoV-2; self-test

## 1. Introduction

The coronavirus disease (COVID-19) pandemic has impacted global health problems also economic and social stability. Therefore, detecting the severe acute respiratory syndrome coronavirus 2 (SARS-CoV-2) is urgently required to trace and break the chain of disease transmission. In addition, several diagnostic strategies are also needed to efficiently evaluate potential cases and disseminate information about population exposure and immunity (Azzi et al. 2021; Mina and Andersen 2021).

Reverse transcription-polymerase chain reaction (RT-PCR) is currently the gold standard test for detecting SARS-CoV-2 despite its limitations, such as the availability of the machine, operators, and reagents, makes the test expensive. Furthermore, there is a significant time lag from the time of sampling to the end decision, causing more possibilities for transmission while waiting for the result (Crozier et al. 2021). Moreover, RT-PCR is not an ideal test tool for mass screening because it can crowd people at the specimen collection point (Azzi et al. 2020b; To et al. 2020b). Furthermore, some regions, especially third-world countries, do not have access to the RT-PCR test (Grant et al. 2021).

Lateral flow immunoassay (LFIA) based on an antigen offers an inexpensive and rapid virus detection. This assay explicitly meets the ASSURED criteria (Afford-

able, Sensitive, Specific, User-friendly, Rapid and Robust, Equipment-free, Deliverable to end-users) (Kosack et al. 2017). Although antigen assays have lower analytical sensitivity than RT-PCR tests, their capacity to detect infectious individuals with culturable viruses is comparable (Mina and Andersen 2021). In addition, the availability of antigen tests based on LFIA has shortened the waiting period for the detection results. This tool can provide quick results and avoid examination-related delays, allowing patients to isolate themselves on time (Crozier et al. 2021). As evidence, Liverpool's epidemic curve declined when paired LFIA based on antigen, and PCR testing was performed (Mina et al. 2021).

On the other hand, the demand for COVID-19 throughput has prompted new collection methods, including saliva (Mina and Andersen 2021), where the SARS-CoV-2 virus has been found in it by several researchers. They collected saliva using various techniques and analyzed it with RT-PCR. The results revealed a sensitivity range of 87% to 100% (Azzi et al. 2020b; To et al. 2020a,b).

Saliva can be an alternative specimen to detect the SARS-CoV-2 and has been categorized as an upper respiratory tract specimen (CDC 2021). Compared to nasopharyngeal and oropharyngeal specimens, the salivary specimen collection process is non-invasive. In addition, the saliva sampling process does not require skilled health workers, so it can minimize costs related to diagnostics and reduce virus transmission to the health workers from accidental exposure to droplets caused by patients who are triggered to sneeze or cough during nasopharyngeal swab sampling (Azzi et al. 2020b; To et al. 2020b; Wyllie et al. 2020).

Further studies have shown that saliva specimens contain saliva secreted from the major or minor salivary glands and contain secretions that descend from the nasopharynx or exit the lungs through the action of cilia lining the airways (To et al. 2020b). In addition, angiotensin-converting enzyme 2 (ACE 2), the main receptor for the entry of SARS-CoV-2 into human body cells, is highly expressed in oral epithelial cells, especially in the tongue (Xu et al. 2020).

As a diagnostic fluid, saliva has several advantages, including saliva that the patient can easily collect, thereby minimizing the risk of transmitting the virus to health workers, and the specimen collection procedure is non-invasive (Azzi et al. 2020b; To et al. 2020b). Another advantage of the saliva specimen is that the viral load profile in saliva containing SARS-CoV-2 almost reaches its peak at symptom onset. Salivary viral load increases in the first week after symptom onset and decreases over time (To et al. 2020a). In addition, SARS-CoV-2 can be detected in saliva for 20 days or longer (To et al. 2020a). Moreover, the detection of SARS-CoV-2 in saliva has low variability compared to nasopharyngeal swabs. Besides, asymptomatic patients can be detected using saliva samples (Wyllie et al. 2020).

Several factors should be considered when developing a rapid test based on LFIA, including the selection of antibodies (Koczula and Gallotta 2016; de Puig et al. 2017), the formulation of a buffer based on the characteristics of the sample, and the optimization of conjugation pH for the orientation of the antibody with the highest antigen capacity (Ruiz et al. 2019). In the lateral flow immunoassay development, it is preferable to use antibodies with a high binding affinity. However, the fastest binding kinetic, which shows how quickly the antibody binds to the antigen to form a complex, is also critical (Biosciences 2017). This binding kinetics is especially important for optimizing the test line because the interaction between antigen with capture antibody will take only a few seconds (Gasperino et al. 2018). Measuring binding kinetics is essential because it reveals the time component of the interaction. This parameter can be measured by surface plasmon resonance (SPR), biolayer interferometry (BLI), and isothermal titration calorimetry (ITC). These methods can provide helpful information about the association and dissociation binding kinetics (Parolo et al. 2020).

Previously, the saliva-based antigen rapid test was developed to detect the viral spike protein. The sensitivity of this assay using the saliva specimen of a confirmed COVID-19 patient was 93%, but its specificity was still low (42%), owing to the high number of false positives (Azzi et al. 2020a). In this study, we developed an LFIA based on an antigen for detecting SARS-CoV-2 nucleocapsid using saliva specimens because nucleocapsid proteins are highly immunogenic and abundant during infection (Dutta et al. 2020). This study aims to develop a saliva-based COVID-19 antigen rapid test by selecting the best antibody using SPR, formulating the running buffer for a saliva sample, and evaluating the antigen detection, including determining the limit of detection of the prototype, specificity using saliva samples that were confirmed negative for COVID-19, and selectivity to the other viral protein.

## 2. Materials and Methods

### 2.1. Material and reagents

IgG anti-N SARS-CoV-2 monoclonal antibody clone 3H11 (Cat. no. A02047) and clone 4H2 (Cat. no.

**TABLE 1** The different composition of running buffer for optimization

| Type of running buffer | Composition |
| --- | --- |
| A | 75 mM sodium phosphate buffer, 1% NaCl, 1% Triton X-100 and 0.02% sodium azide |
| B | 75 mM sodium phosphate buffer, 1% NaCl, 1% Triton X-100, 0.5% N-acetyl-L-cysteine, and 0.02% sodium azide |
| C | 75 mM sodium phosphate buffer, 1% NaCl, 1% Triton X-100, 0.025 M EDTA and 0.02% sodium azide |
| D | 75 mM sodium phosphate buffer |

A02048), SARS-CoV-2 nucleocapsid (N) protein (Cat. no. Z03488), and Biotin L protein (Cat. no. M00097) were obtained from Genscript (USA). Tetrachloroauric (III) acid (HAuCl$_4$, 99.99%) was obtained from Sigma Aldrich (USA). Bovine serum albumin was obtained from Sigma Aldrich (USA). All reagents were of analytical or chemical purity. For lateral flow test strips, sample pad and absorbent pad were obtained from Ahlstrom-Munksjo, the conjugate pad was obtained from GE Healthcare (Germany), and fast nitrocellulose membrane was obtained from MDI membrane technology and backing cards.

## 2.2. The measurement of antibody binding kinetics

The measurement of binding kinetics was carried out using Nano SPR. The antibody was immobilized on the gold plate surface using covalent linking with 3-Mercaptopropionic acid and N-(*3-Dimethylaminopropyl)-N'-ethyl carbodiimide hydrochloride* (EDC): N-Hydroxysuccinimide (NHS) (1:1), with the flow rate 25 µL/min. The bovine serum albumin (1%) was flowed to reduce or eliminate non-specific responses. The nucleocapsid of SARS-CoV-2 was then flowed to the device at a 100 ng/mL concentration. After obtaining the sensorgram, the association binding kinetics ($k_{on}$) was calculated.

## 2.3. The synthesis of gold nanoparticles

Gold nanoparticles (AuNP) were synthesized by the thermal citrate reduction method described in previous work (Dong et al. 2020). The HAuCl$_4$ solution (0.5 mM) was heated to 90 ºC with constant stirring. Then, 2 mL of 1.5% trisodium citrate (with a temperature approximately equal to that of HAuCl$_4$ solution) was added to the solution rapidly. The solution mixture was kept heated at 90 ºC for 30 min after the solution turned wine red. AuNP solutions were characterized using a UV-Vis spectrophotometer at a wavelength of 400-800 nm. Particle size (nm) was measured using a Malvern Zetasizer (Malvern Instrument Ltd, UK).

## 2.4. The conjugation of AuNP and IgG anti-N SARS-CoV-2

### 2.4.1 pH optimization

The AuNP solution was adjusted to pH 7.5 until 9.0 using 0.3 M potassium carbonate (K$_2$CO$_3$). Then, 200 µL of each solution was placed in a 1.5 mL microtube, followed by the addition of 20 µL IgG anti-N SARS-CoV-2, which has diluted in 10 mM borate buffer, which has the same pH as AuNP. The solution was incubated with constant stirring at 600 rpm at room temperature for 30 min. Each microtube was added with 10% NaCl solution, then allowed to stand for 5 min. AuNP aggregation occurs when the solution changes color from red to purple.

### 2.4.2 Minimum concentration of antibody optimization for conjugation

The AuNP solution was adjusted to the optimized pH. Then, 200 µL of each solution was placed in a 1.5 ml microtube, followed by the addition of 20 µL IgG anti-N SARS-CoV-2 in different concentrations. The solution was incubated with constant stirring at 600 rpm at room temperature for 30 min. Each microtube was added with 10% NaCl solution, then allowed to stand for 5 min. AuNP aggregation occurs when the solution changes color from red to purple.

### 2.4.3 Preparation of AuNP-IgG anti-N SARS-CoV-2 conjugate

The AuNP was conjugated to SARS-CoV-2 anti-N IgG at the the optimized pH and minimum concentration accord-
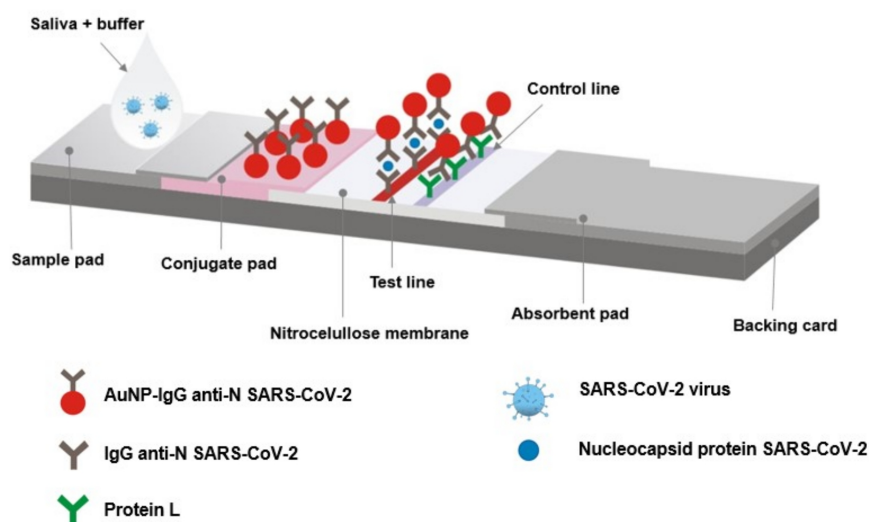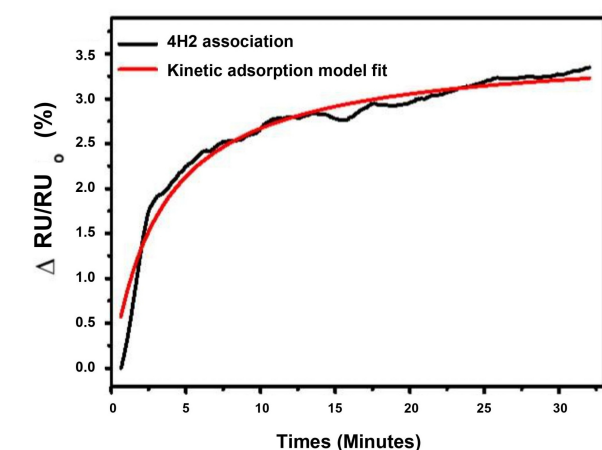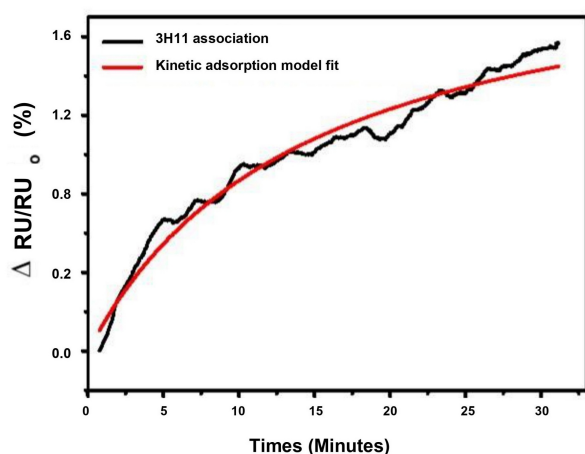


**FIGURE 1** Schematic illustration of saliva-based antigen rapid test detection.

ing to the conjugation method (Parolo et al. 2020) with slight modifications. A total of 100 µL IgG anti-N SARS-CoV-2 (in 10 mM borate buffer) was added to 1 mL of AuNP solution that had been adjusted for pH using 0.3 M potassium carbonate. The mixture was incubated with constant stirring at 600 rpm at room temperature for 30 min and then centrifuged at 14000 rpm at 4 ºC for 20 min. The pellets were resuspended using 2 mM borate buffer and 10% bovine serum albumin (BSA; final concentration of BSA in solution was 1%), then incubated with constant stirring at 600 rpm at room temperature for 30 min. The solutions were centrifuged at 14000 rpm 4 ºC for 20 min. Finally, the conjugate was resuspended with a conjugate diluent (2 mM borate buffer containing 0.5% BSA, 5% sucrose, 5% trehalose, and 0.095% sodium azide). The final product was characterized using a UV-Vis spectrophotometer and stored at 4 ºC in a dark container.
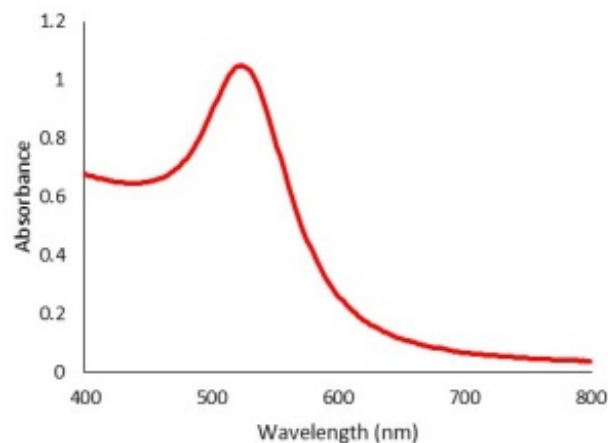
### 2.5. Preparation of saliva samples

Saliva (posterior oropharyngeal saliva) is taken by coughing first and then spitting it into a collecting container (sputum pot). It is advisable to take saliva in the morning and not eat or drink for 30 min before saliva is collected. The saliva used in this study was the saliva that was confirmed negative by PCR. This study was approved by the Research Ethics Commission of the Ministry of Education and Culture, Padjadjaran University, with the number 860/UN6.KEP/EC/2020 dated September 15th, 2020.

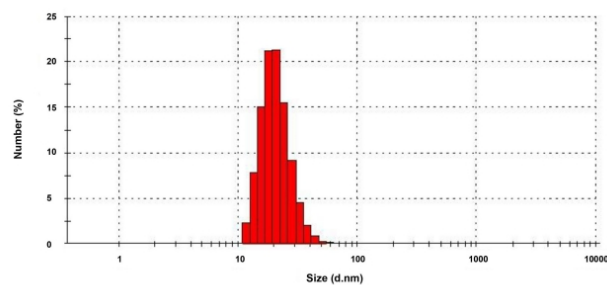### 2.6. Preparation of lateral flow immunoassay test strip

The sample pad was blocked by 10 mM Tris buffer pH 8.0, 0.2% casein, 0.05% Tween 20 and adjusted until reached pH 8, then dried for 1 h by vacuum drying. The dried sample pad was mounted on a strip containing a dried conjugate pad, nitrocellulose membrane, and an absorbent pad, as shown in Figure 1.

### 2.7. Antigen Detection Performing

Saliva was diluted in the running buffer with the dilution ratio of 3:5 (saliva: running buffer), then 70 µL of the mixture was applied to the sample pad. The signal was observed on the test line and control line for 15 min. The test was also carried out by adding N protein to the saliva and

(a)

(b)

**FIGURE 2** Sensorgram of SPR binding kinetics of (a) IgG anti-N SARS-CoV-2 clone 4H2 with N protein, and (b) IgG anti-N SARS-CoV-2 clone 3H11 with N protein. Clone 4H2 demonstrated 2.5 times faster association binding kinetics than clone 3H11, indicating that clone 4H2 binds to the antigen and forms a complex faster than clone 3H11.

(a)

(b)

**FIGURE 3** (a) UV-Vis spectrum of AuNP and (b) AuNP's particle size distribution.

buffer (the final concentration of N protein is 1 µg/mL). The running buffer optimization was also performed in different compositions (Table 1). The optimum running buffer is then optimized at different pH.

Different concentrations of N protein were tested to find out what is the smallest concentration of N protein can be detected by a developed saliva-based antigen test. For specificity, the saliva samples have been confirmed negative by RT-PCR. For selectivity, the recombinant protein of hemagglutinin (HA) avian influenza virus was tested to the developed saliva-based antigen test.

## 3. Results and Discussion

### 3.1. The kinetic binding of IgG anti-N SARS-CoV-2

The antibodies characterized in this study were IgG anti-N SARS-CoV-2 (mAb) clone 3H11 and IgG anti-N SARS-CoV-2 (mAb) clone 4H2, while the antigen used was the nucleocapsid protein SARS-CoV-2. The measurement using Nano-SPR showed that IgG anti-N SARS-CoV-2 clone 4H2 had association binding kinetics of 2.5 times faster ($k_{on} = 2.08 \times 10^4$ M$^{-1}$ s$^{-1}$) compared to IgG anti-N SARS-CoV-2 clones 3H11 ($k_{on} = 8.16 \times 10^3$ M$^{-1}$ s$^{-1}$), this demonstrates that clone 4H2 binds to the antigen to form a complex more quickly than clone 3H11 (Figure 2). So, clone
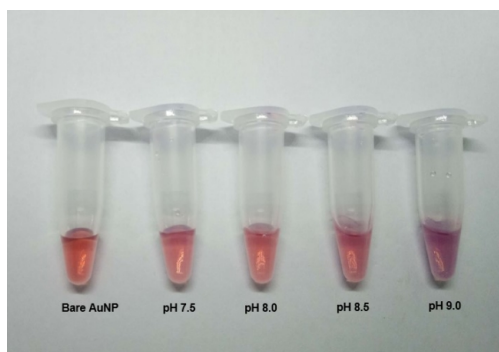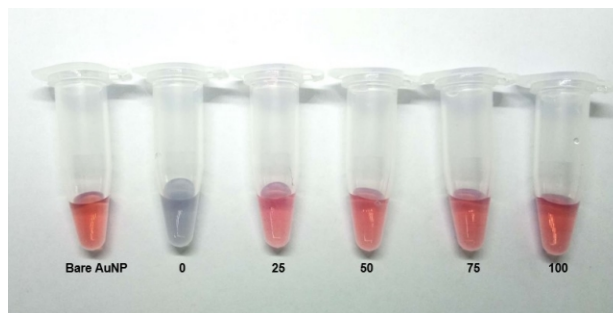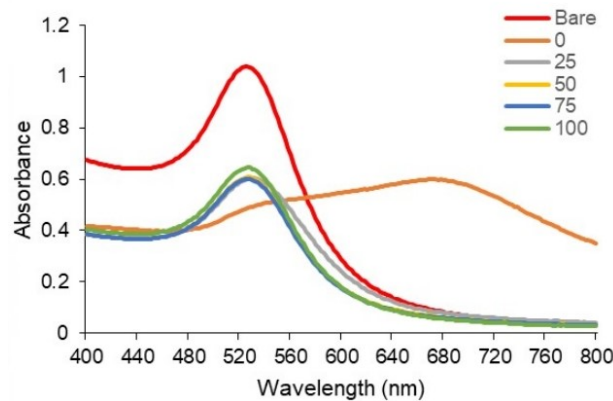


(a)
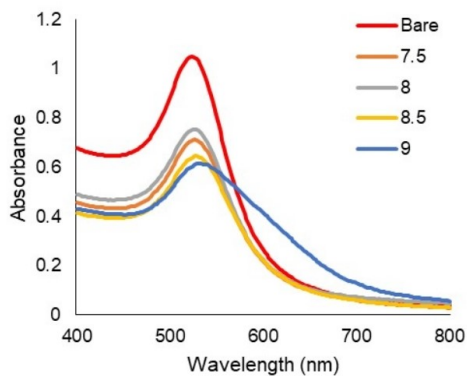


(b)

**FIGURE 4** (a) The color change of the AuNP-IgG anti-N SARS-CoV-2 clone 3H11 conjugate solution after the addition of 10% NaCl (b) and its UV-Vis spectra at various pH.

(a)



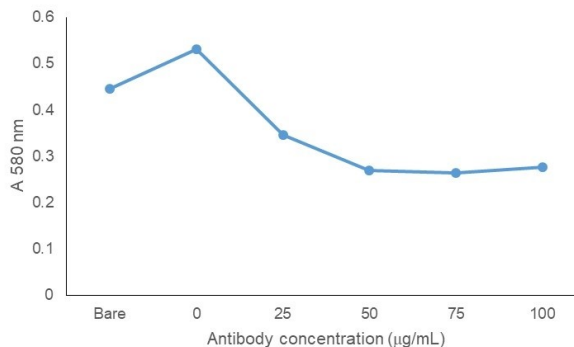(b)



(c)

**FIGURE 5** (a) The color change of the AuNP-IgG anti-N SARS-CoV-2 clone 3H11 conjugate solution after the addition of 10% NaCl (b) and its UV-Vis spectra at various concentration (c) the flocculation curve of AuNP-IgG anti-N SARS-CoV-2 clone 3H11 with various concentrations of antibody at a wavelength of 580 nm.

4H2 could be used as a capture antibody, while clone 3H11 was used as a detection antibody or an antibody conjugated with AuNP.

### 3.2. Characterization of the synthesis of gold nanoparticles

Figure 3 shows UV-Vis absorption spectra and the average and particle size distribution of AuNP. The maximum ultraviolet absorption peak of AuNPs was measured at 524 nm. The synthesized AuNPs have the highest intensity (21.4%), with the size particle around 21.04 nm.
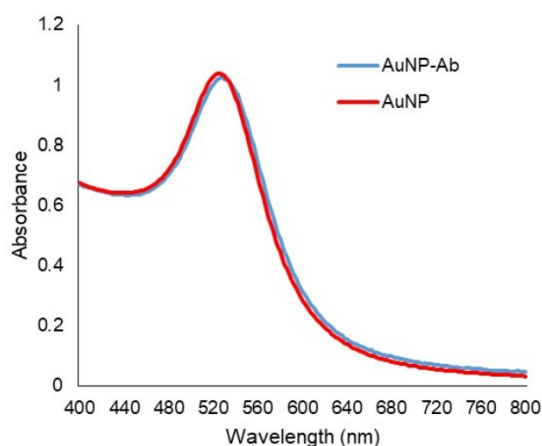
**FIGURE 6** UV-Vis spectrum of AuNP before and after conjugation with IgG anti-N SARS-CoV-2 clone 3H11.

### 3.3. pH optimization for conjugation

The pH of the colloidal gold nanoparticles and the number of antibodies is important factors in the conjugate preparation process. The conjugation was tested at 10 mM borate buffer at various pH to determine the optimal value. Visual observations showed that the pH 7.5, 8.0, and 8.5 conjugates colors were not changed, while the 9.0 conjugates were changed from red to purple. This color change is due to aggregation, which is caused by unstable AuNPs.

Figure 4 shows UV-Vis absorption spectra of various pH. These spectra can be used to monitor the stability of nanoparticle solutions. As the particles become unstable, the peak frequently broadens, and there is a significant wavelength shift due to aggregate formation, as evidenced by the shape of the absorbance peak at pH 9.0. The absorbance of the particles was also decreased as a result of the depletion of stable nanoparticles, indicating that pH 8.0 is a pH that can stabilize nanoparticles.

### 3.4. Minimum concentration of antibody optimization for conjugation

Besides pH, the concentration of antibodies conjugated with AuNP influences conjugate stability. The results showed that at a concentration of 0 μg/mL and 25 μg/mL the conjugate solution's color was changed after adding 10% NaCl. These color changes were caused by the formation of aggregates due to the addition of an electrolyte. In this condition, the amount of added antibodies was insufficient to stabilize AuNP. If the concentration of antibody added is sufficient to stabilize AuNP, the solution will not change color (Hermanson 2008), as shown in solutions with concentrations of 50, 75, and 100 μg/mL (Figure 5).
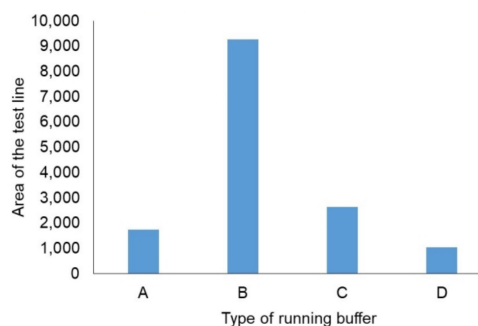
UV-Vis absorption spectra of various concentrations are shown in Figure 5a. The shape of the absorbance peak at concentration 0 μg/mL is wider than the shape of the absorbance peak at other concentrations, showing the presence of aggregation caused by the instability of the suspen-
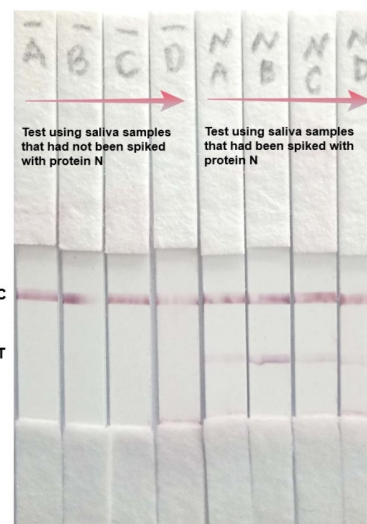


(a)
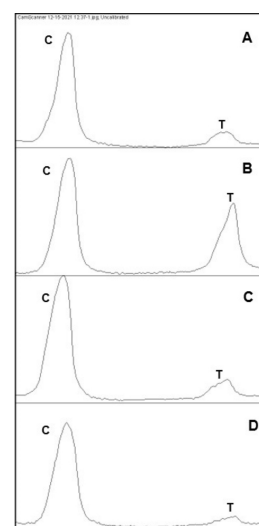


(b)



(c)

**FIGURE 7** (a) Saliva-based antigen rapid test result of various running buffer composition. C = control line, T = test line. The composition of running buffer is as follow: A: 75 mM sodium phosphate buffer, 1% NaCl, 1% Triton X-100 and 0.02% sodium azide; B: 75 mM sodium phosphate buffer, 1% NaCl, 1% Triton X-100, 0.5% N-acetyl-L-cysteine, and 0.02% sodium azide; C: 75 mM sodium phosphate buffer, 1% NaCl, 1% Triton X-100, 0.025 M EDTA and 0.02% sodium azide; and D: 75 mM sodium phosphate buffer. (b) The ImageJ results of the saliva-based antigen rapid test result of various running buffer composition, and (c) the area histogram on the test line.

**(a)**



**(b)**



**(c)**
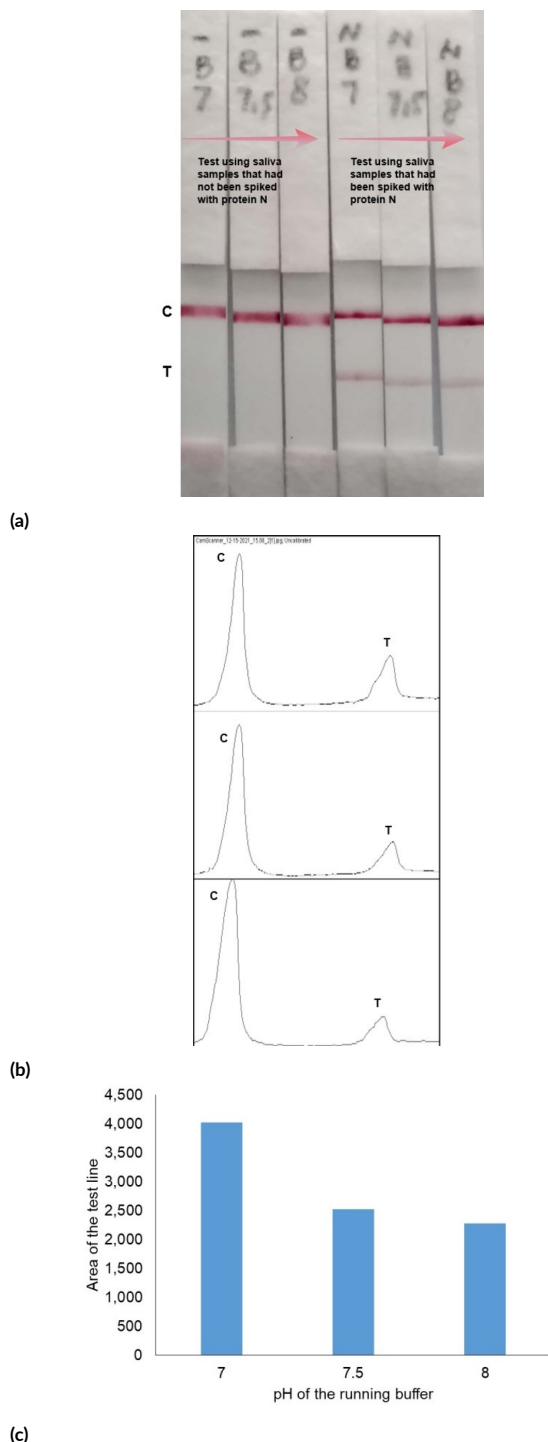
**FIGURE 8** (a) Saliva-based antigen rapid test result of various pH of the running buffer, (b) the ImageJ result, and (c) the area histogram on the test line. C = control line, T= test line.

sion due to the addition of 10% NaCl. The absorbance at 580 nm was also measured to determine the minimum concentration used in the conjugation process. An increase in absorbance at 580 nm indicates aggregation in the solution (Byzova et al. 2017; Parolo et al. 2020). Because of electrostatic, hydrophobic, and Van der Waals interactions, the addition of antibodies to AuNPs results in spontaneous adsorption on the surface of gold particles. Because antibody

molecules are bound to the AuNP surface, the conjugate will be stable and will not coagulate if the absorbance at 580 nm decreases (Hermanson 2008).

In Figure 5c, the absorbance at 580 nm was increased from bare AuNP to antibody concentration of 0 μg/mL. At concentrations of 25 μg/mL, the absorbance begins to decline, then gradually increases to concentrations of 50 μg/mL, and finally stabilizes at concentrations of 75 μg/mL and 100 μg/mL. As can be seen, a concentration of antibodies of 50 μg/mL is a stabilization point and the minimum concentration of antibodies capable of stabilizing AuNP. The antibody concentration used for AuNP-IgG conjugation was 10% higher than the antibody concentration at the stabilization point (Hermanson 2008). Thus, the minimum concentration used in the AuNP-IgG conjugation process is 55 μg/mL.

### 3.5. The conjugation of AuNP-IgG anti-N SARS-CoV-2

AuNP-IgG anti-N SARS-CoV-2 clone 3H11 conjugation was performed at a pH of 8.0 and an antibody concentration of 55 μg/mL. The UV-Vis absorption spectra showed a shift in wavelength from 524 nm to 528 nm (Figure 6).

### 3.6. Optimization of the running buffer

The running buffer was optimized with various compositions. The buffer compositions used in the study were: (A) 75 mM sodium phosphate buffer, 1% NaCl, 1% Triton X-100 and 0.02% sodium azide; (B) 75 mM sodium phosphate buffer, 1% NaCl, 1% Triton X-100, 0.5% N-acetyl-L-cysteine, and 0.02% sodium azide; (C) 75 mM sodium phosphate buffer, 1% NaCl, 1% Triton X-100, 0.025 M EDTA and 0.02% sodium azide; and (D) 75 mM sodium phosphate buffer. The tests using saliva samples that had not been spiked with protein N revealed that all running buffers produced signals on the control line but not on the test line, so it was concluded that all buffers did not provide non-specific interactions on the developed saliva-based antigen test system.

The test results using saliva samples spiked with N protein with a final concentration of 1 μg/mL showed that running buffer B produced a stronger signal on the test and control lines after 15 minutes compared to another running buffer (Figure 7). The signal that appears on the test line is then quantified using the ImageJ application, and running buffer B produces the largest area on the test line than the area in running buffers A, C, and D. This showed that the addition of mucolytic agent to the running buffer could reduce the viscosity of saliva and improving its sensitivity.

The buffer was then optimized with various pH. The test results using saliva samples spiked with N protein with a final concentration of 1 μg/mL showed that all running buffers produced a thin signal on the test line after 15 minutes. The signal on the test line is then quantified using the ImageJ application. Running buffer B with pH 7 produces the largest area on the test line than running buffer B with pH 7.5 and 8.0 (Figure 8). This result demonstrated that the greater the ionic strength of the buffer, the lower the sensitivity.

**(a)**



**(b)**



**(c)**
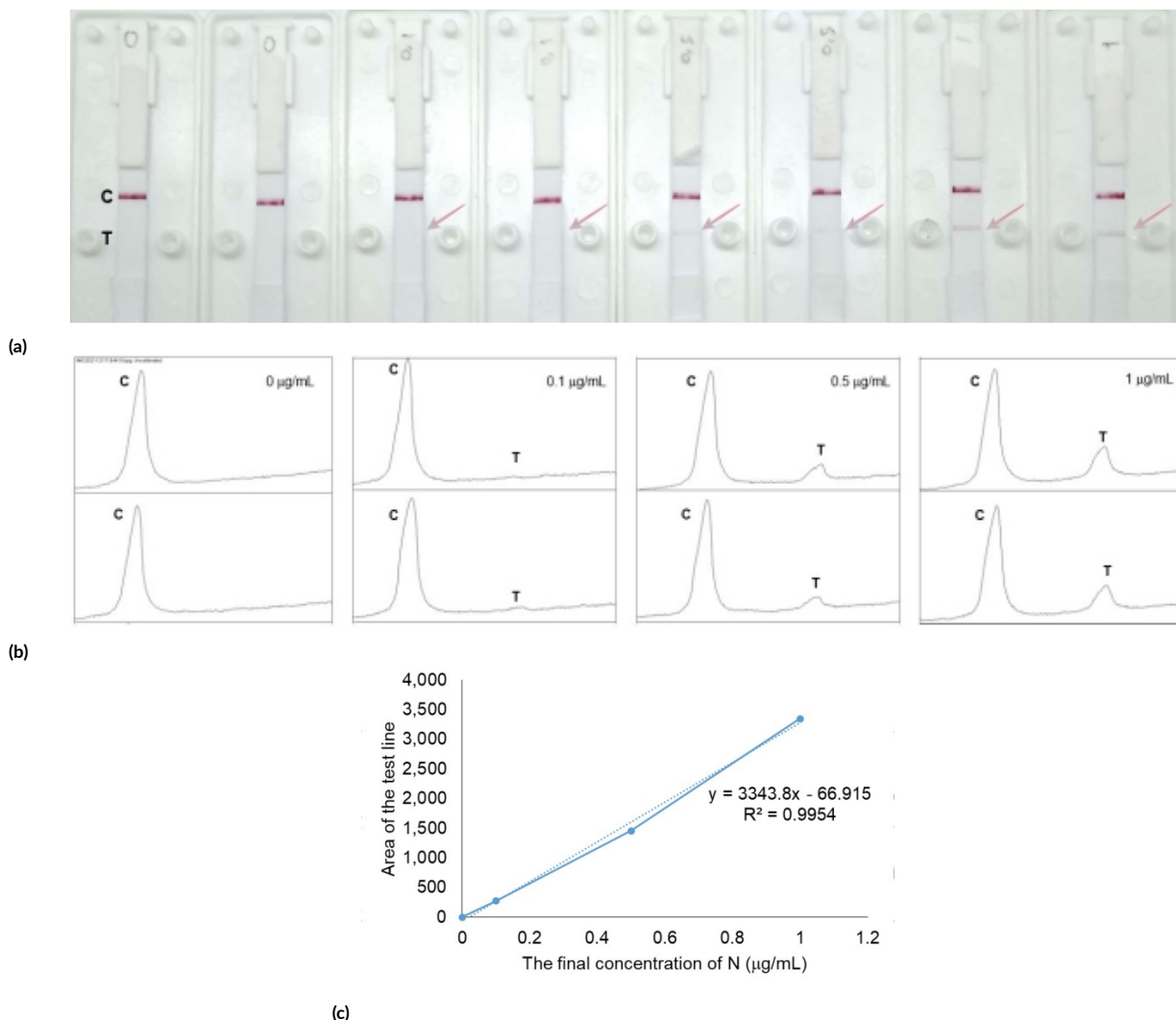
**FIGURE 9** (a) Antigen detection performed using various N protein concentrations showed the saliva-based antigen rapid test could detect the N protein at 0.1 µg/mL, (b) the ImageJ result, and (c) the area histogram on the test line showed that resulted was linear, with an R2 value of 0.9954. C = control line, T= test line.

### 3.7. The smallest concentration of N protein was detected by a developed saliva-based antigen test.

The developed saliva-based antigen test prototype was tested with saliva spiked with N protein at various concentrations. The final concentration of N protein was 0 µg/mL, 0.1 µg/mL, 0.5 µg/mL, 1 µg/mL. A developed saliva-based antigen test prototype could detect N protein with the smallest concentration of 0.1 µg/mL. The signal on the test line was quantified using the ImageJ application. The resulting area graph showed linearity with R2 = 0.9954 (Figure 9).



**FIGURE 10** LFIA of saliva samples which confirm negative COVID-19 by RT-PCR by using developed saliva-based rapid antigen, showed that there were no lines in the test line. This indicated that the assay was specific for COVID-19. C = control line, T= test line.

### 3.8. The specificity and selectivity of the developed saliva-based antigen test

The specificity tests were carried out using 10 saliva samples confirmed negative for COVID-19, and the results showed 100% true negative (Figure 10). We also evaluated the selectivity using a recombinant hemagglutinin protein of the avian influenza virus was tested with a concentration of as much as 1 mg/mL. The test results did not show any signal on the test line (Figure 11), showing no cross-reaction with it.

### 3.9. The comparison between developed saliva-based antigen rapid test and commercialized antigen test.
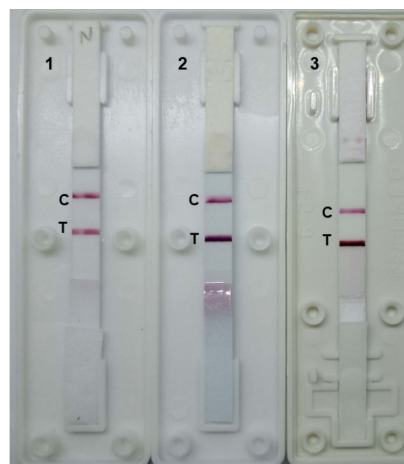
The prototype of the developed saliva-based antigen rapid test was then compared with the commercialized product which is the nasopharyngeal swab-based antigen rapid test, to determine the performance of the assays to detect 20 µg/mL N protein. The N protein was spiked into the saliva specimen for saliva-based rapid antigen and spiked into the nasopharyngeal specimen for nasopharyngeal swab-based antigen rapid test CePAD® and Abbot®. The commercialized products were used as a control for the developed saliva-based antigen rapid test. The developed saliva-based antigen rapid test produces a less strong signal on the test line than the commercialized antigen rapid test (Figure 12). This result indicates that the created test's sensitivity is still below expectations and that there is still an opportunity for improvement by using antibodies with improved binding kinetics.

### 3.10. Discussion

In this work, a few points must be considered to get better sensitivity, including the selection of antibodies, the size of AuNP, the minimal non-specific binding (NSB), and the running buffer formulation. The selection of antibodies is critical to empirically testing the available pairs to determine which pair performs the best (de Puig et al. 2017).
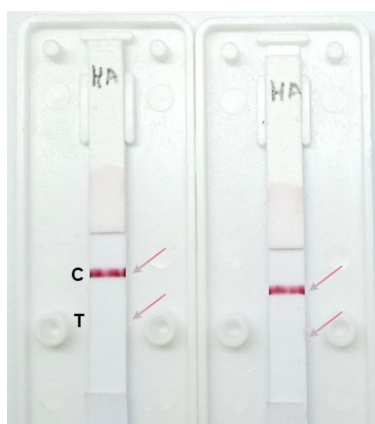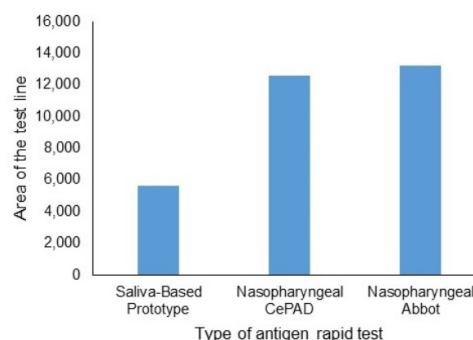
**FIGURE 11** The developed saliva-based antigen rapid test using recombinant HA protein of avian influenza virus, showed that there were no line in the test line. This indicated that the assay was no cross reaction. The test was performed duplo. C = control line, T= test line.

(a)
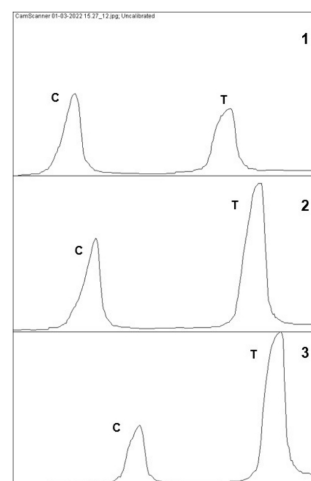
(b)

(c)

**FIGURE 12** (a) The comparison of the antigen detection performed of developed saliva-based antigen rapid test and commercialized antigen rapid test using 20 µg/mL N protein. The commercialized antigen rapid test is used as a control for developed saliva-based antigen rapid test (a). 1 = developed saliva-based rapid antigen, 2 = nasopharyngeal CePAD®, 3 = nasopharyngeal Abbot®. The N protein is spiked into the saliva specimen for saliva-based rapid antigen and spiked into nasopharyngeal specimen for nasopharyngeal CePAD® and nasopharyngeal Abbot®. (b) The ImageJ results. (c) The area histogram on the test line of various antigen rapid test. When compared to the nasopharyngeal swab-based antigen rapid test, the saliva-based antigen rapid test produces a weaker signal on the test line. C = control line, T= test line.

This pair of antibodies can be determined which one is the detection antibody and which is the capture antibody based on the fastest antigen binding kinetics. The capture antibody must have a faster binding kinetic because the interaction with the analyte is in a few seconds when the flow passes through the test line area. Meanwhile, the detection antibody has a longer time to bind to the analyte when the flow passes through the conjugate pad to the test line (Parolo et al. 2020). SPR could measure the binding kinetics of the antigen that binds to the antibody immobilized on the surface of the SPR sensor (Miyazaki et al. 2017). In this experiment, we can determine the antibody which has the fast association binding kinetics, which tells us how quickly the antibody binds to the antigen to form a complex. This selection is very important to improve the sensitivity because it is a major issue in the development of LFIA. Therefore, the antibodies must be pure and carefully designed because it is an important step to obtaining good sensitivity and specificity in the assay system (Koczula and Gallotta 2016). It is very important to select antibodies that are specific for use in the lateral flow assay.

According to dynamic light scattering (DLS), the synthesized AuNP were monodispersed with the size particle around 21.04 nm. These small AuNPs have a small surface area for antibody internalization (Byzova et al. 2017). Moreover, the AuNP with size 26 ± 6 nm was also used to develop LFIA of cortisol in saliva, which has an analytical sensitivity of 73% (Panfilova 2021).

The nitrocellulose membrane used in this developed LFIA was the fastest membrane due to the viscosity of saliva. In addition, the use of blocking agents such as BSA and casein together with surfactants can reduce the NSB between the AuNP and the antibody immobilized in the test line. The blocking agent was added into the conjugate AuNP-IgG anti-N SARS-CoV-2, conjugate pad, and sample pad and is proven to reduce the NSB (O'Farrell 2009; Parolo et al. 2020).

The running buffer formulation was considered by the characteristics of saliva, which contains a lot of water, inorganic compounds, and organic compounds (Pfaffe et al. 2011). The saliva is more viscous than water because it contains a lot of mucins. The presence of mucin in saliva can interfere with the SARS-CoV-2 virus detection process because mucin is the main structural component of mucus that makes saliva viscous (Frenkel and Ribbeck 2015). This viscosity prevents saliva from flowing in the rapid test device. So, the sample needs to be treated to reduce viscosity by adding a mucolytic agent that can cleavage the intermolecular and intramolecular disulfide bonds of mucin (Carlson et al. 2018). Four running buffers were used for optimization as listed above in the Results section. Figure 7 demonstrates that running buffer B is the best choice, and we can conclude that the type of running buffer may affect the sensitivity of LFIA. N-acetyl-L-cysteine has been shown to increase the signal intensity in the test line, and this is because saliva can flow rapidly along the membrane. The pH of the running buffer was also optimized. Figure 8 demonstrates that the running buffer B with pH 7 is the best choice, and we conclude that the pH also may affect the sensitivity of the developed LFIA.

The antigen detection was performed in various concentrations of N protein. The linear graph showed that the linearity of the test has a good result with a value of $R^2 = 0.9954$. And the smallest concentration of N protein that was detected by developed LFIA was 0.1 μg/mL. The developed LFIA produced half the signal intensity of the commercial nasopharyngeal swab-based antigen rapid test. This result shows that the developed test's sensitivity is still under expectation, and there is still room for improvement by using antibodies with better binding kinetics. We do not have access to the better antibodies that are suitable for lateral flow assay, considering antibodies that were purchased are meant for ELISA-based detection. The specificity was also tested using the avian influenza virus's recombinant hemagglutinin protein, which revealed no cross-reaction. In addition, when the developed LFIA was performed on negative saliva samples, high specificity (100%) was also demonstrated.

## 4. Conclusions

The pair of IgG anti-N SARS-CoV-2 for detecting nucleocapsid in the sandwich-format of developed saliva-based antigen rapid test was characterized by SPR to determine the association kinetic binding rate of antibody, and it revealed that IgG anti-N SARS-CoV2 clone 4H2 as a capture antibody, and IgG anti-N SARS-CoV-2 clone 3H11 as the detection antibody. The optimum condition for conjugation of developed saliva-based antigen rapid test is at pH 8 in 10 mM borate buffer with IgG anti-N SARS-CoV-2 clone 3H11 concentration at 55 μg/mL. The best formulation of running buffer is 75 mM sodium phosphate buffer, 1% NaCl, 1% Triton X-100, 0.5% N-acetyl-L-cysteine, and 0.02% sodium azide at pH 8. The application of N-acetyl-L-cysteine in the buffer has been demonstrated can increase the signal strength in the test line and reduce the viscosity of saliva. The developed LFIA can detect the nucleocapsid antigen at 0.1 μg/mL, and show no cross-reaction with avian influenza virus hemagglutinin. We can conclude that all kinds of treatments in the experiment could increase the signal. The advantage of the developed saliva-based antigen rapid test is providing an early diagnosis of COVID-19, allowing patients to choose to isolate directly at home and receive prompt treatment. This assay can be performed on a daily, and it can help to reduce the spread of the SARS CoV-2 virus because the sampling and examination of the sample will not involve other people.

## Acknowledgments

## Authors' contributions

SS performed and designed the experiments, wrote the original draft, reviewed and edited the paper. DS helped perform the experiments. SSY, FG, and HC helped design the experiments. MY, TS designed the experiments, analyzed and interpreted the data, wrote and reviewed the paper. BA, AY designed the experiments and contributed the materials. NF, HLW, LW, and BA designed the experiments and performed the clinical RT-PCR test.

## Competing interests

The authors declare no conflict of interest.

## References

Azzi L, Baj A, Alberio T, Lualdi M, Veronesi G, Carcano G, Ageno W, Gambarini C, Maffioli L, Saverio SD, Gasperina DD, Genoni AP, Premi E, Donati S, Azzolini C, Grandi AM, Dentali F, Tangianu F, Sessa F, Maurino V, Tettamanti L, Siracusa C, Vigezzi A, Monti E, Iori V, Iovino D, Ietto G, Grossi PA, Tagliabue A, Fasano M. 2020a. Rapid salivary test suitable for a mass screening program to detect SARS-CoV-2: A diagnostic accuracy study. J. Infect. 81(3):e75–e78. doi:10.1016/j.jinf.2020.06.042.

Azzi L, Carcano G, Gianfagna F, Grossi P, Gasperina DD, Genoni A, Fasano M, Sessa F, Tettamanti L, Carinci F, Maurino V, Rossi A, Tagliabue A, Baj A. 2020b. Saliva is a reliable tool to detect SARS-CoV-2. J. Infect. 81(1):e45–e50. doi:10.1016/j.jinf.2020.04.005.

Azzi L, Maurino V, Baj A, Dani M, D'Aiuto A, Fasano M, Lualdi M, Sessa F, Alberio T. 2021. Diagnostic salivary tests for SARS-CoV-2. J. Dent. Res. 100(2):115–123. doi:10.1177/0022034520969670.

Biosciences I. 2017. Guide to Lateral Flow Immunoassays p. 1–15. URL https://fnkprddata.blob.core.windows.net/domestic/.

Byzova NA, Safenkova IV, Slutskaya ES, Zherdev AV, Dzantiev BB. 2017. Less is more: A comparison of antibody-gold nanoparticle conjugates of different ratios. Bioconjug. Chem. 28(11):2737–2746. doi:10.1021/acs.bioconjchem.7b00489.

Carlson TL, Lock JY, Carrier RL. 2018. Engineering the Mucus Barrier. Annu. Rev. Biomed. Eng. 20(1):197–220. doi:10.1146/annurev-bioeng-062117-121156.

Crozier A, Rajan S, Buchan I, McKee M. 2021. Put to the test: Use of rapid testing technologies for COVID-19. BMJ 372:1–7. doi:10.1136/bmj.n208.

de Puig H, Bosch I, Gehrke L, Hamad-Schifferli K. 2017. Challenges of the nano–bio interface in lateral low and dipstick immunoassays. Trends Biotechnol. 35(12):1169–1180. doi:10.1016/j.tibtech.2017.09.001.

Dong J, Carpinone PL, Pyrgiotakis G, Demokritou P, Moudgil BM. 2020. Synthesis of precision gold nanoparticles using Turkevich method. KONA Powder Part. J. 37:224–232. doi:10.14356/kona.2020011.

Dutta NK, Mazumdar K, Gordy JT. 2020. The nucleocapsid protein of SARS–CoV-2: A target for vaccine development. J. Virol. 94(13):e00647–20. doi:10.1128/jvi.00647-20.

Frenkel ES, Ribbeck K. 2015. Salivary mucins in host defense and disease prevention. J. Oral Microbiol. 7(1):29759. doi:10.3402/jom.v7.29759.

Gasperino D, Baughman T, Hsieh HV, Bell D, Weigl BH. 2018. Improving lateral flow assay performance using computational modeling. Annu. Rev. Anal. Chem. 11(1):219–244. doi:10.1146/annurev-anchem-061417-125737.

Grant BD, Anderson CE, Alonzo LF, Garing SH, Williford JR, Baughman TA, Rivera R, Glukhova VA, Boyle DS, Dewan PK, Weigl BH, Nichols KP. 2021. A SARS-CoV-2 coronavirus nucleocapsid protein antigen-detecting lateral flow assay. PLoS One 16(11):e0258819. doi:10.1371/journal.pone.0258819.

Hermanson GT. 2008. Bioconjugate Techniques. London: Academic Press is an imprint of Elsevier. doi:10.1016/B978-0-12-370501-3.X0001-X.

Koczula KM, Gallotta A. 2016. Lateral flow assays. Essays Biochem. 60(1):111–120. doi:10.1042/EBC20150012.

Kosack CS, Page AL, Klatser PR. 2017. A guide to aid the selection of diagnostic tests. Bull. World Health Organ. 95(9):639–645. doi:10.2471/BLT.16.187468.

Mina MJ, Andersen KG. 2021. COVID-19 testing: One size does not fit all. Science 371(6525):126–127. doi:10.1126/science.abe9187.

Mina MJ, Peto TE, García-Fiñana M, Semple MG, Buchan IE. 2021. Clarifying the evidence on SARS-CoV-2 antigen rapid tests in public health responses to COVID-19. Lancet 397(10283):1425–1427. doi:10.1016/S0140-6736(21)00425-6.

Miyazaki CM, Shimizu FM, Ferreira M. 2017. Surface Plasmon Resonance (SPR) for Sensors and Biosensors. Elsevier Inc. doi:10.1016/B978-0-323-49778-7/00006-0.

O'Farrell B. 2009. Evolution in Lateral Flow–Based Immunoassay Systems. New York, USA: Humana Press, a part of Springer Science-Business Media. doi:10.1007/978-1-59745-240-3_1.

Panfilova E. 2021. Development of a prototype lateral flow immunoassay of cortisol in saliva for daily monitoring of stress. Biosensors 11(5):146. doi:10.3390/bios11050146.

Parolo C, Sena-Torralba A, Bergua JF, Calucho E, Fuentes-Chust C, Hu L, Rivas L, Álvarez-Diduk R, Nguyen EP, Cinti S, Quesada-González D, Merkoçi A. 2020. Tutorial: Design and fabrication of nanoparticle-based lateral-flow immunoassays. Nat. Protoc. 15(12):3788–3816. doi:10.1038/s41596-020-0357-x.

Pfaffe T, Cooper-White J, Beyerlein P, Kostner K, Pun-

yadeera C. 2011. Diagnostic potential of saliva: Current state and future applications. Clin. Chem. 57(5):675–687. doi:10.1373/clinchem.2010.153767.

Ruiz G, Tripathi K, Okyem S, Driskell JD. 2019. pH impacts the orientation of antibody adsorbed onto gold nanoparticles. Bioconjug. Chem. 30(4):1182–1191. doi:10.1021/acs.bioconjchem.9b00123.

To KKW, Tsang OTY, Leung WS, Tam AR, Wu TC, Lung DC, Yip CCY, Cai JP, Chan JMC, Chik TSH, Lau DPL, Choi CYC, Chen LL, Chan WM, Chan KH, Ip JD, Ng ACK, Poon RWS, Luo CT, Cheng VCC, Chan JFW, Hung IFN, Chen Z, Chen H, Yuen KY. 2020a. Supplementary Appendix. Lancet Diabetes Endocrinol. 6736(20):1–7. doi:10.1016/S1473-3099(20)30196-1.

To KKW, Tsang OTY, Yip CCY, Chan KH, Wu TC, Chan JMC, Leung WS, Chik TSH, Choi CYC, Kandamby DH, Lung DC, Tam AR, Poon RWS, Fung AYF, Hung IFN, Cheng VCC, Chan JFW, Yuen KY. 2020b. Consistent detection of 2019 novel coronavirus in saliva. Clin. Infect. Dis. 71(15):841–843. doi:10.1093/cid/ciaa149.

Wyllie AL, Fournier J, Casanovas-Massana A, Campbell M, Tokuyama M, Vijayakumar P, Geng B, Muenker MC, Moore AJ, Vogels CBF, Petrone ME, Ott IM, Lu P, Lu-Culligan A, Klein J, Venkataraman A, Earnest R, Simonov M, Datta R, Handoko R, Naushad N, Sewanan LR, Valdez J, White EB, Lapidus S, Kalinich CC, Jiang X, Kim DJ, Kudo E, Linehan M, Mao T, Moriyama M, Oh JE, Park A, Silva J, Song E, Takahashi T, Taura M, Weizman OE, Wong P, Yang Y, Bermejo S, Odio C, Omer SB, Cruz CSD, Farhadian S, Martinello RA, Iwasaki A, Grubaugh ND, Ko AI. 2020. Saliva is more sensitive for SARS-CoV-2 detection in COVID-19 patients than nasopharyngeal swabs. medRxiv (2):1–12. doi:10.1101/2020.04.16.20067835.

Xu H, Zhong L, Deng J, Peng J, Dan H, Zeng X, Li T, Chen Q. 2020. High expression of ACE2 receptor of 2019-nCoV on the epithelial cells of oral mucosa. Int. J. Oral Sci. 12(1):8. doi:10.1038/s41368-020-0074-x.